Kinetics and Mechanism of the Gas Phase Reaction of Atomic Chlorine with CH_2ICl at 206−432 K

M. Bilde, J. Sehested, and O. J. Nielsen

Atmospheric Chemistry, Building 313, Plant Biology and Biogeochemistry Department, Risø National Laboratory, DK-4000 Roskilde, Denmark

T. J. Wallington,* R. J. Meagher, and M. E. McIntosh

Ford Research Laboratory, SRL-3083, Ford Motor Company, P.O. Box 2053, Dearborn, Michigan 48121-2053

C. A. Piety,† J. M. Nicovich,‡ and P. H. Wine*,†,‡,§

Georgia Institute of Technology, Atlanta, Georgia 30332

Received: June 3, 1997; In Final Form: August 12, 1997[⊗]

The title reaction was studied using two different experimental techniques: laser flash photolysis with resonance fluorescence detection of Cl atoms and continuous photolysis with FTIR detection of end products. Over the temperature range 206−432 K the rate constant for reaction of Cl atoms with CH_2ICl is given (to within ±15%) by the Arrhenius expression $k_1 = 4.4 \times 10^{-11} \exp(195/T)$ cm^3 molecule^{-1} s^{-1}, which gives $k_1 = 8.5 \times 10^{-11}$ cm^3 molecule^{-1} s^{-1} at 298 K. Variation of the total pressure of N_2 diluent over the range 5−700 Torr at 295 K had no discernible (<10%) effect on the rate of reaction. At 295 K in 100−700 Torr of N_2 the reaction proceeds via iodine transfer to give CH_2Cl radicals. As part of this work the rate constant $k(CH_2Cl+O_2+M)$ was measured at 295 K in the presence of 1−800 Torr of N_2 diluent. The results were well described by the Troe expression with a broadening factor F_c of 0.6 and limiting low- and high-pressure rate constants of $k_0 = (1.8 \pm 0.1) \times 10^{-30}$ cm^6 molecule^{-2} s^{-1} and $k_\infty = (3.3 \pm 0.3) \times 10^{-12}$ cm^3 molecule^{-1} s^{-1}. The results are discussed with respect to the available literature for reactions of Cl atoms with halogenated organic compounds and the potential role of the title reaction in atmospheric chemistry.

1. Introduction

The atmospheric chemistry of iodine is a topic of current interest. It has been suggested that iodine chemistry may influence the HO_2/OH and NO_2/NO concentration ratios and hence the oxidizing capacity of the troposphere.[1,2] Unlike the corresponding chlorinated and brominated compounds, iodocompounds and reservoir species such as ICl are easily photodissociated in the near UV and visible part of the electromagnetic spectrum. As a consequence, iodine in its various forms is rapidly converted to iodine atoms, which can take part in ozone depleting cycles in the troposphere and lower stratosphere.[3]

The oceans are the main source of iodine, and CH_3I has generally been regarded as the main carrier of marine iodine to the atmosphere. However, recent studies indicate that the source strength for CH_3I may be exceeded by the source strength of other iodocompounds such as CH_2ICl, CH_2I_2, and C_2H_5I. Moore and Tokarczyk[4] and Class and Ballschmiter[5] report concentrations of CH_2ICl of 0.1−3.8 ng/L in surface seawater in the northwestern Atlantic and suggest that iodine carried from the ocean to the atmosphere by CH_2ICl may be as important as that carried by CH_3I. The atmospheric photodissociation rates of CH_3I, C_2H_5I, and CH_2ICl have been investigated recently[6,7] and range from days to hours.

To assess the roles played by CH_3I, CH_2ICl, and CH_2I_2 in atmospheric chemistry kinetic and mechanistic information concerning their reactions with atmospherically relevant species is needed. In partial fulfillment of this need we report here the results of a study of the reaction of Cl atoms with CH_2ICl.

$$Cl + CH_2ICl \rightarrow \text{products} \qquad (1)$$

Absolute kinetic data were obtained using the laser flash photolysis facility at Georgia Institute of Technology. Relative rate and product studies were performed at Ford Motor Company using a FTIR-smog chamber system.

2. Experimental Section

The experimental systems used are described in detail elsewhere.[8,9] The uncertainties reported in this paper are two standard deviations unless otherwise stated. Standard error propagation methods are used to calculate combined uncertainties.

2.1. FTIR−Smog Chamber System. The FTIR−smog chamber experiments were carried out at Ford Motor Company. The FTIR system was interfaced to a 140 liter Pyrex reactor. Radicals were generated by the UV irradiation (22 black lamps) of mixtures of CH_2ICl, Cl_2, C_2H_4, C_2H_6, and CH_3Cl in 700 Torr total pressure with N_2, O_2, or air diluent at 295 K. Reagent concentrations used were CH_2ICl, 0−47.2 mTorr; Cl_2, 99−2090 mTorr; C_2H_4, 0−4.9 mTorr; C_2H_6, 0−42.9 mTorr; and CH_3Cl, 0−45 mTorr. Loss of reactants and the formation of products were monitored by FTIR spectroscopy, using an analyzing path length of 27 m and a resolution of 0.25 cm^{-1}. Infrared spectra were derived from 32 coadded spectra. CH_2ICl, CH_3Cl, and CH_2Cl_2 were monitored using their characteristic features over the wavenumber range 700−1500 cm^{-1}. Reference spectra were acquired by expanding known volumes of reference materials into the reactor.

† School of Chemistry and Biochemistry.
‡ Georgia Tech Research Institute.
§ School of Earth and Atmospheric Sciences.
⊗ Abstract published in *Advance ACS Abstracts,* October 1, 1997.

S1089-5639(97)01796-9 CCC: $14.00

2.2. Laser Flash Photolysis−Resonance Fluorescence Setup. Chlorine atom kinetics in the presence of varying amounts of CH_2ICl were studied at Georgia Institute of Technology (Georgia Tech) using a laser flash photolysis (LFP)−resonance fluorescence (RF) apparatus.[9] Chlorine atoms were produced by 355 nm laser flash photolysis of Cl_2. Third harmonic radiation from a Quanta Ray Model DCR-2 Nd:YAG laser provided the photolytic light source. The photolysis laser could deliver up to 1×10^{17} photons/(6 ns) pulse at a repetition rate of up to 10 Hz. Fluences employed in this study ranged from 20 to 50 mJ cm^{-2} $pulse^{-1}$.

To avoid accumulation of photochemically generated reactive species, all experiments were carried out under "slow flow" conditions. The linear flow rate through the reactor was typically 3 cm s^{-1} while the laser repetition rate was varied over the range 5−10 Hz (it was 5 Hz in most experiments). Since the direction of flow was perpendicular to the photolysis laser beam, no volume element of the reaction mixture was subjected to more than a few laser shots. Molecular chlorine (Cl_2), CH_2ICl, and CF_2Cl_2 flowed into the reaction cell from 12 L Pyrex bulbs containing dilute mixtures in nitrogen buffer gas, while N_2 flowed directly from its high-pressure storage tank; the bulb containing CH_2ICl was blackened to prevent photolysis by room lights. The gas mixtures and additional N_2 were premixed before entering the reaction cell. Concentrations of each component in the reaction mixture were determined from measurements of the appropriate mass flow rates and the total pressure. The fraction of CH_2ICl in the CH_2ICl/N_2 mixture was checked frequently by UV photometry at 254 nm using a mercury penray lamp as the light source. It was determined that $\sigma_{CH_2ICl}(254\ nm) = 8.3 \times 10^{-19}$ cm^2 $molecule^{-1}$ (base e) in good agreement with the recent work by Rattigan et al.[6]

The gases used in this study had the following stated minimum purities: N_2, 99.999%; Cl_2, 99.9%;[10] CF_2Cl_2, 99.9%.[10] Nitrogen was used as supplied, while Cl_2 and CF_2Cl_2 were degassed at 77 K before being used to prepare mixtures with N_2. The liquid CH_2ICl sample had a stated minimum purity of 97%. It was transferred under nitrogen atmosphere into a vial fitted with a high vacuum stopcock and then degassed repeatedly at 77 K before being used to prepare mixtures with N_2.

3. Results

3.1. Relative Rate Study of the Reaction of Cl Atoms with CH_2ICl. Relative rate experiments were performed using the FTIR system to investigate the kinetics of the reaction of Cl atoms with CH_2ICl. The techniques used are described elsewhere.[11] Reaction mixtures consisted of 2−33 mTorr of CH_2ICl, 4−43 mTorr of the reference compound (C_2H_4 or C_2H_6), and 0.3−0.5 Torr of Cl_2 in 5−700 Torr of either O_2 or N_2 diluent. Photolysis of molecular chlorine was the source of chlorine atoms.

$$Cl_2 + h\nu \rightarrow 2Cl \qquad (2)$$

The kinetics of reaction 1 were measured relative to reactions 3 and 4.

$$Cl + CH_2ICl \rightarrow \text{products} \qquad (1)$$

$$Cl + C_2H_4 \rightarrow \text{products} \qquad (3)$$

$$Cl + C_2H_6 \rightarrow C_2H_5 + HCl \qquad (4)$$

The observed loss of CH_2ICl versus the losses of C_2H_4 and C_2H_6 in the presence of Cl atoms is shown in Figure 1. Sensitivity toward three different experimental conditions was tested by varying one parameter at a time. First, the initial concentration of CH_2ICl was varied over the range 2−33 mTorr. Second, the total pressure of N_2 diluent was varied over the range 5−700 Torr. Third, experiments were performed in either 700 Torr of N_2 or O_2 diluent. The results are shown in Figure 1 and were invariant to changes in the initial concentration of CH_2ICl, total pressure, and type of diluent gas.

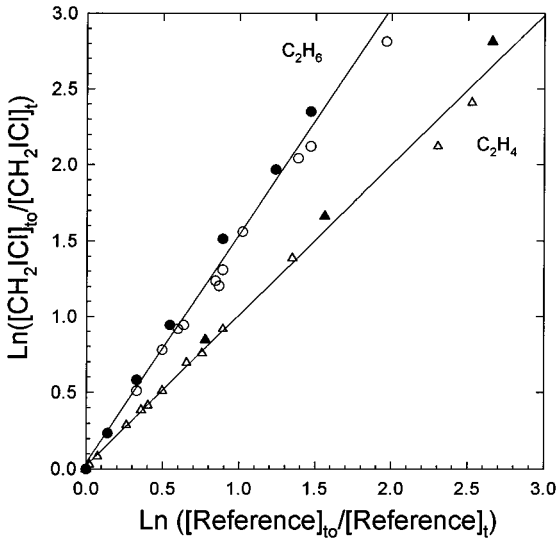

Figure 1. Decay of CH_2ICl versus the decays of C_2H_6 (circles) and C_2H_4 (triangles) when mixtures containing these compounds were exposed to Cl atoms in 5−700 Torr of N_2 (open symbols) or O_2 (filled symbols) diluent.

Linear least-squares analysis gives $k_1/k_3 = 0.99 \pm 0.06$ and $k_1/k_4 = 1.50 \pm 0.15$. Using $k_3 = 9.29 \times 10^{-11}$ and $k_4 = 5.7 \times 10^{-11}$ cm^3 $molecule^{-1}$ s^{-1} [12] gives $k_1 = (9.2 \pm 0.6) \times 10^{-11}$ and $(8.6 \pm 0.9) \times 10^{-11}$, respectively. We estimate that potential systematic errors associated with uncertainties in the reference rate constants could add an additional 10% to the uncertainty ranges for k_1. Propagating this additional uncertainty gives values of $k_1 = (9.2 \pm 1.1) \times 10^{-11}$ and $(8.6 \pm 1.2) \times 10^{-11}$ cm^3 $molecule^{-1}$ s^{-1}. We choose to cite a final value which is an average of the two determinations with error limits which encompass the extremes of the individual determinations. Hence $k_1 = (8.9 \pm 1.5) \times 10^{-11}$ cm^3 $molecule^{-1}$ s^{-1} independent of total pressure over the range 5−700 Torr. As seen from Table 1 this result is in excellent agreement with those obtained using the laser flash photolysis apparatus described in the following section.

TABLE 1: Summary of Kinetic Data for the Cl + CH_2ICl Reaction Obtained Using the LFP−RF Technique[a]

T	P	$[Cl_2]$	$[Cl]_{t=0}$	$[CH_2ICl]_{max}$	no. of expts[b]	k'_{max}	$k_1 \pm 2\sigma$[c]
432	50	68	1.1	726	8	5130	6.92 ± 0.17
350	50	20−100	0.5−1.5	760	10	6060	7.67 ± 0.35
298	50	68	1.3	469	7	3780	8.04 ± 0.20
297	20	65	1.7	230	3	2100	8.74 ± 1.06
297	20	65	1.7	234	3	2190	8.93 ± 1.12[d]
260	50	55	1.1	588	9	5790	9.67 ± 0.38
232	50	65	1.2	537	6	5360	10.0 ± 0.2
206	50	37	1.0	722	11	8290	11.4 ± 0.3

[a] Units: T (K), P (Torr), concentrations (10^{11} molecules cm^{-3}), k'_{max} (s^{-1}), k_1(10^{-11} cm^3 $molecule^{-1}$ s^{-1}). [b] Expt ≡ determination of one pseudo-first-order rate coefficient. [c] Errors represent precision only. [d] 1.0 × 10^{15} CF_2Cl_2 cm^{-3} added to the reaction mixture.

3.2. LFP−RF Study of the Temperature Dependence of the Reaction of Cl Atoms with CH_2ICl. In all LFP−RF experiments, chlorine atoms were generated by laser flash photolysis of Cl_2 at 355 nm:

$$Cl_2 + h\nu(355\ nm) \rightarrow nCl(^2P_{3/2}) + (2-n)Cl(^2P_{1/2}) \quad (5)$$

The fraction of chlorine atoms generated in the excited spin−orbit state, $Cl(^2P_{1/2})$, is thought to be very small, i.e., less than 0.01.[13,14] Recently, it has been reported that the rate coefficient for $Cl(^2P_{1/2})$ quenching by N_2 is slower than previously thought, i.e., 5.0×10^{-15} cm^3 molecule^{-1} s^{-1}.[15] However, on the basis of reported rate coefficients for $Cl(^2P_{1/2})$ deactivation by saturated halocarbons (all gas kinetic except CF_4),[15−18] we expect that the rate coefficient for $Cl(^2P_{1/2})$ deactivation by CH_2ICl is very fast, i.e., faster than the observed Cl+CH_2ICl reaction rate. Hence, it seems safe to assume that all Cl+CH_2ICl kinetic data are representative of an equilibrium mixture of $Cl(^2P_{1/2})$ and $Cl(^2P_{3/2})$. As a further check on the assumption of spin state equilibration, the rate coefficient at $T = 297$ K and $P = 20$ Torr was measured with and without CF_2Cl_2, a very efficient $Cl(^2P_{1/2})$ quencher,[15,17,18] added to the reaction mixture; as expected, this variation in experimental conditions had no effect on the observed reaction rate (see Table 1). Finally, it should be noted that at 355 nm the absorption cross section of Cl_2 is 2 orders of magnitude larger than that of CH_2ICl[7,12] and for the experimental conditions employed here the photolysis of CH_2ICl will be of negligible importance.

All LFP−RF experiments were carried out under pseudo-first-order conditions with CH_2ICl in large excess over Cl. Hence, in the absence of side reactions that remove or produce chlorine atoms, the Cl temporal profile following the laser flash is described by the relationship

$$\ln\{[Cl]_o/[Cl]_t\} = (k_1[CH_2ICl] + k_6)t = k't \quad (I)$$

where k_1 and k_6 are the rate coefficients for the reactions

$$Cl + CH_2ICl \rightarrow \text{products} \quad (1)$$

$$Cl \rightarrow \text{first-order loss by diffusion from the detector field of view} \quad (6)$$

and/or reaction with background impurities

The bimolecular rate coefficients of interest $k_1(P,T)$ are determined from the slopes of k' versus $[CH_2ICl]$ plots for data obtained at constant P and T. Typical data observed in the LFP−RF experiments are shown in Figures 2 and 3. Well-behaved pseudo-first-order kinetics were observed at all temperatures and pressures investigated, i.e., Cl temporal profiles obeyed equation I, and k' increased linearly with increasing $[CH_2ICl]$ but was independent of laser fluence and Cl_2 concentration. Such observations suggest that reactions 1 and 6 are, indeed, the only processes that significantly affect the Cl time history. Measured bimolecular rate coefficients $k_1(P,T$ are summarized in Table 1. We find that reaction 1 is very fast and has a negative activation energy, i.e., k_1 increases with decreasing temperature. An Arrhenius plot for reaction 1 is shown in Figure 4. The best fit Arrhenius expression is

$$k_1 = (4.4 \pm 0.6) \times 10^{-11} \exp((195 \pm 34)/T)\ \text{cm}^3\ \text{molecule}^{-1}\ \text{s}^{-1}$$

Uncertainties in the Arrhenius expression are 2σ and represent precision only. The accuracy of measured values of $k_1(P,T)$ is estimated to be ±15% at all temperatures and pressures within the range investigated, i.e., 206−432 K and 20−50 Torr.

The photochemical system used in the LFP−RF experiments appears to be relatively free of complications from unwanted side reactions which could destroy or regenerate chlorine atoms.

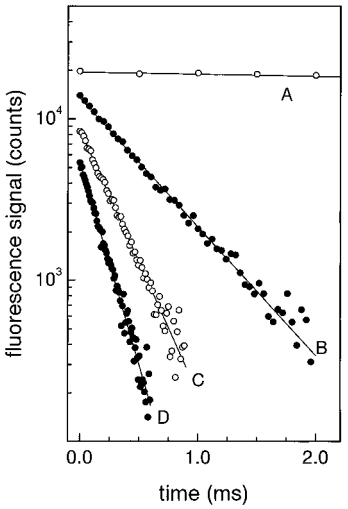

Figure 2. Typical $Cl(^2P_J)$ temporal profiles observed in the LFP−RF studies. Experimental conditions: $T = 260$ K and $P = 50$ Torr. $[Cl_2] = 5.5 \times 10^{12}$ molecules cm^{-3}; $[Cl]_{t=0} = 1.1 \times 10^{11}$ atoms cm^{-3}; $[CH_2ICl]$ in units of 10^{13} molecules cm^{-3} = (A) 0.00, (B) 2.04, (C) 3.82, and (D) 5.88; number of laser shots averaged = (A) 100, (B) 1000, (C) 1500, and (D) 2000. Solid lines are obtained from least-squares analyses and give the following pseudo-first-order decay rates in units of s^{-1} = (A) 28, (B) 1840, (C), 3760, and (D) 5790.

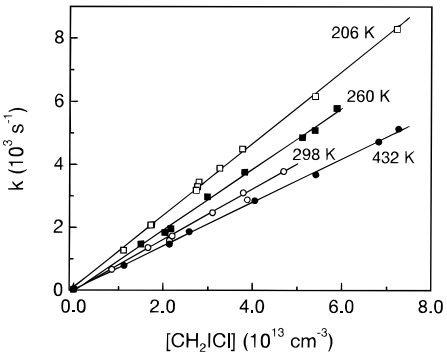

Figure 3. Plots of k', the $Cl(^2P_J)$ pseudo-first-order decay rate, versus CH_2ICl concentration from data obtained at four different temperatures over the range 206−432 K. Solid lines are obtained from linear least squares analyses; the slopes of these lines give the bimolecular rate coefficients summarized in Table 1.

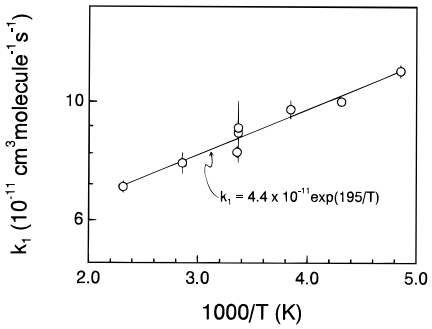

Figure 4. Arrhenius plot for the $Cl(^2P_J)$+CH_2ICl reaction. The solid line is obtained from a linear least-squares analysis which weights each data point equally; it represents the Arrhenius expression shown in the figure (units are cm^3 molecule $^{-1}$ s^{-1}).

Radical concentrations were sufficiently low that radical−radical reactions could not possibly be important. As reported in section 3.4, the radical product of reaction 1 is CH_2Cl. Hence, one secondary reaction which warrants consideration is Cl regeneration via

$$CH_2Cl + Cl_2 \rightarrow CH_2Cl_2 + Cl \quad (7)$$

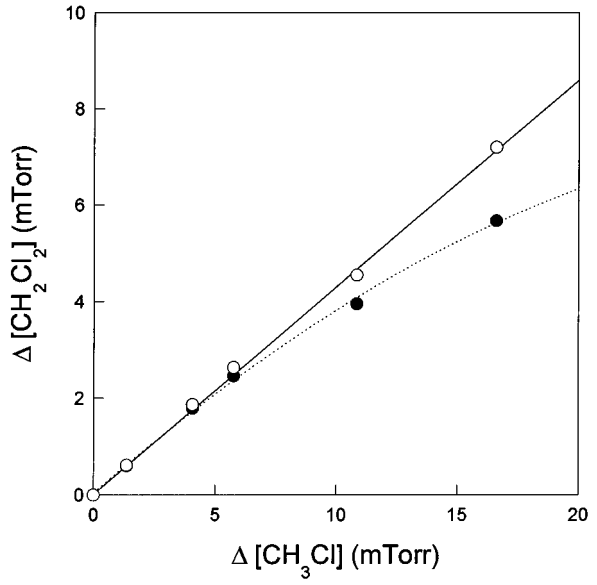

Figure 5. Formation of CH_2Cl_2 versus loss of CH_3Cl following UV irradiation of a mixture of 34 mTorr of CH_3Cl, 2.04 Torr of Cl_2, 0.324 Torr of O_2, in 700 Torr of N_2 diluent. Filled symbols are the observed data; open symbols are data corrected for loss of CH_2Cl_2 via reaction with Cl atoms.

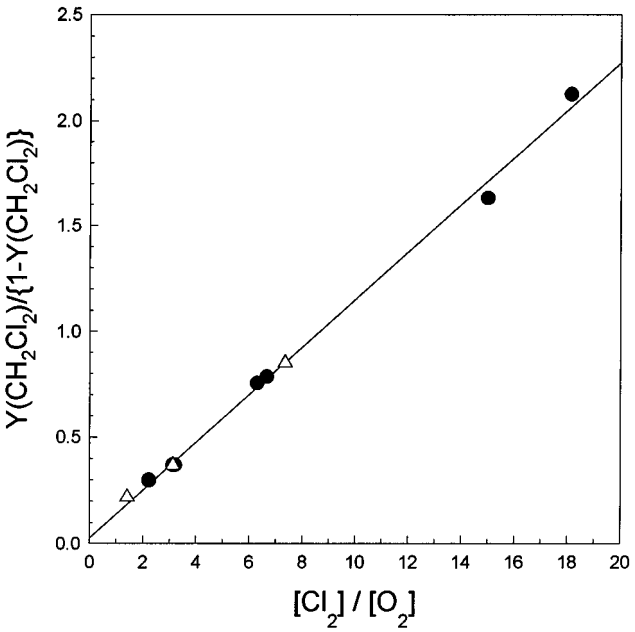

Figure 6. Plot of $y(CH_2Cl_2)/\{1 - y(CH_2Cl_2)\}$ versus $[Cl_2]/[O_2]$ for experiments using $CH_3Cl/Cl_2/O_2/N_2$ mixtures (circles) and $CH_2ICl/Cl_2/O_2/N_2$ mixtures (triangles). All experiments were performed at 700 Torr total pressure.

Over the temperature range of our study, reaction 7 is rather slow, i.e., $k_7 = (2.9 \pm 1.0) \times 10^{-13}$ cm^3 molecule^{-1} s^{-1} for 200 K < T < 400 K.[19] Given the low Cl_2 concentrations employed in the LFP−RF experiments (see Table 1), we would expect reaction 7 to have no measurable effect on observed Cl temporal profiles. The results from experiments at 350 K, where the observed kinetics were unaffected by a factor of 5 variation in Cl_2 concentration, confirm this expectation.

3.3. Study of the Relative Reactivity of CH_2Cl Radicals toward O_2 and Cl_2. Prior to investigating the products and mechanism of the reaction of Cl atoms with CH_2ICl, the competition between reactions 7 and 8 was studied as a function of total pressure using the FTIR−smog chamber setup.

$$CH_2Cl + Cl_2 \rightarrow CH_2Cl_2 + Cl \quad (7)$$

$$CH_2Cl + O_2 + M \rightarrow CH_2ClO_2 + M \quad (8)$$

CH_2Cl radicals were generated by the reaction of Cl atoms with CH_3Cl. Photolysis of molecular chlorine was used as a source of chlorine atoms.

$$Cl_2 + h\nu \rightarrow 2Cl \quad (2)$$

$$Cl + CH_3Cl \rightarrow HCl + CH_2Cl \quad (9)$$

Mixtures of 16−45 mTorr of CH_3Cl, 0.2−2.2 Torr Cl_2, and 0−970 mTorr of O_2 in 1−800 Torr N_2 diluent were subjected to UV irradiation, and the formation of CH_2Cl_2 and loss of CH_3Cl were monitored. The filled symbols in Figure 5 show the formation of CH_2Cl_2 following the UV irradiation of a mixture of 34 mTorr of CH_3Cl, 2.04 Torr of Cl_2, 0.324 Torr of O_2, in 700 Torr of N_2 diluent. We ascribe the curvature seen in Figure 5 to secondary loss of CH_2Cl_2 via reaction 10

$$Cl + CH_2Cl_2 \rightarrow HCl + CHCl_2 \quad (10)$$

Corrections for the loss of CH_2Cl_2 via reaction 10 were computed using the Acuchem chemical modeling program[20] with a mechanism consisting of reactions 7, 9, and 10 with $k_9 = 4.9 \times 10^{-13}$ and $k_{10} = 3.3 \times 10^{-13}$ cm^3 molecule^{-1} s^{-1}.[12] The slope of a linear least-squares fit to the corrected data in Figure 5 (open symbols) gives a CH_2Cl_2 yield, $y(CH_2Cl_2)$, of 43 ± 2%.

The rate constant ratio k_7/k_8 can be determined using the following expression:

$$\frac{y(CH_2Cl_2)}{1 - y(CH_2Cl_2)} = \frac{k_7\,[Cl_2]}{k_8\,[O_2]}$$

Figure 6 shows a plot of $y(CH_2Cl_2)/(1 - y(CH_2Cl_2))$ versus the concentration ratio $[Cl_2]/[O_2]$ at 700 Torr total pressure. The circles in Figure 6 are the data obtained from experiments employing $CH_3Cl/Cl_2/O_2/N_2$ mixtures. The line in Figure 6 is a linear least-squares fit to these data which has a slope of 0.112 ± 0.006, hence, $k_8/k_7 = 8.90 \pm 0.49$. This result is consistent, within the combined experimental uncertainties, with the ratio of the reported individual determinations of $k_8 = 2.9 \times 10^{-12}$ (at 700 Torr)[21] and $k_7 = 2.9 \times 10^{-13}$ cm^3 molecule^{-1} s^{-1}[19] which gives $k_8/k_7 = 10$.

Analogous experiments were performed to measure the rate constant ratio k_8/k_7 at total pressures of N_2 diluent of 1−800 Torr at 295 K. The results are shown in Figure 7. The solid line is a fit of the Troe expression[22] given below to the experimental data.

$$\frac{k_8}{k_7} = \frac{k_0[M]}{1 + k_0[M]/k_\infty}\, 0.6^{(1+[\log_{10}(k_0[M]/k_\infty)]^2)^{-1}}$$

From the fit we obtain low- and high-pressure limits for k_8/k_7 of (6.1 ± 0.3) × 10^{-18} cm^3 molecule^{-1} and (11.3 ± 0.9) × 10^{-18} cm^3 molecule^{-1}, respectively. These results can be placed upon an absolute basis using $k_7 = 2.9 \times 10^{-13}$ cm^3 molecule^{-1} s^{-1} [19] which gives $k_{8,0} = (1.8 \pm 0.1) \times 10^{-30}$ cm^6 molecule^{-2} s^{-1} and $k_{8,\infty} = (3.3 \pm 0.3) \times 10^{-12}$ cm^3 molecule^{-1} s^{-1}, which are in excellent agreement with the previous determinations of gives $k_{8,0} = 1.9 \times 10^{-30}$ cm^6 molecule^{-2} s^{-1} and $k_{8,\infty} = 2.9 \times 10^{-12}$ cm^3 molecule^{-1} s^{-1} at 295 K by Fenter et al.[21]

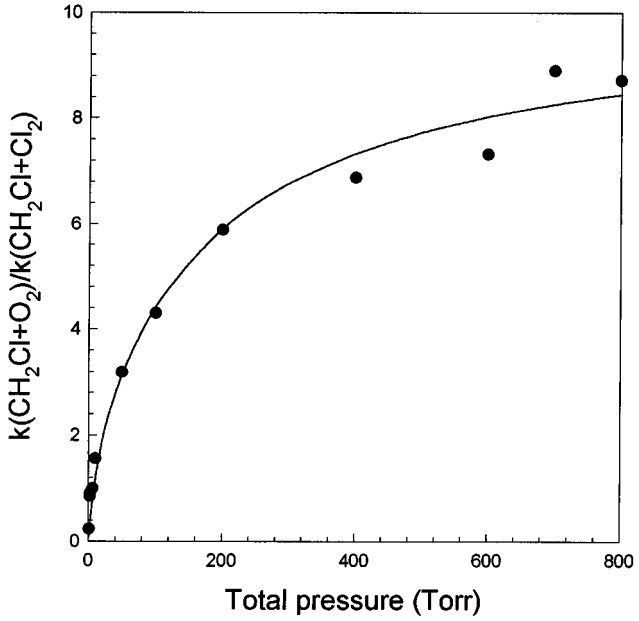

Figure 7. Plot of k_8/k_7 versus total pressure ($T = 295$ K). The solid line is a Troe fit.

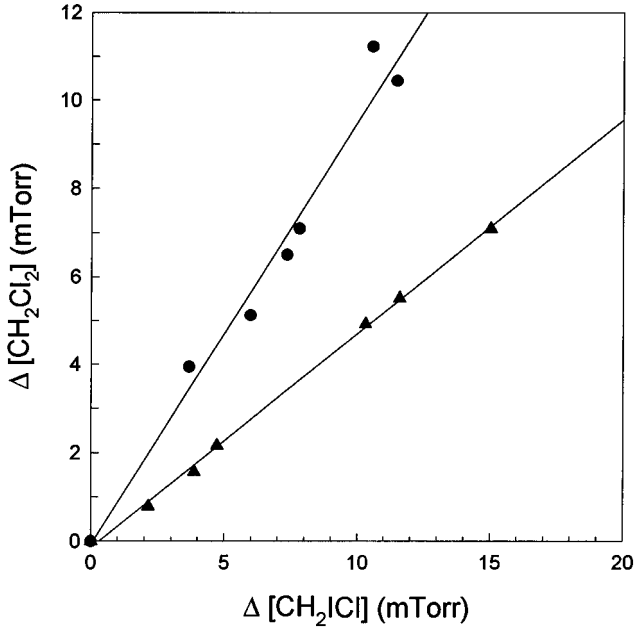

Figure 8. Yield of CH_2Cl_2 versus loss of CH_2ICl following irradiation of $CH_2ICl/Cl_2/N_2$(•) and $CH_2ICl/Cl_2/O_2/N_2$(▲) mixtures at a total pressure of 100 Torr; see text for details.

3.4. Products of the Reaction of Cl Atoms with CH_2ICl. The aim of the experiments presented in this section was to investigate the relative importance of the possible reaction channels 1a−c.

$$CH_2ICl + Cl \rightarrow CHICl + HCl \quad (1a)$$

$$CH_2ICl + Cl \rightarrow CH_2Cl_2 + I \quad (1b)$$

$$CH_2ICl + Cl \rightarrow CH_2Cl + ICl \quad (1c)$$

Mixtures of Cl_2/CH_2ICl in either 100 or 700 Torr total pressure of N_2 diluent with and without added O_2 were irradiated in the FTIR−smog chamber system. The loss of CH_2ICl and the formation of products were monitored by FTIR spectroscopy. In the first experiment a mixture of 46 mTorr of CH_2ICl and 0.2 Torr of Cl_2 in 100 Torr of N_2 diluent was subject to UV irradiation. CH_2Cl_2 was the only carbon containing product observed. The circles in Figure 8 show the observed formation of CH_2Cl_2 versus the loss of CH_2ICl in this experiment. Linear least-squares analysis gives a CH_2Cl_2 yield of 96 ± 14%. The observation of a CH_2Cl_2 yield of essentially 100% shows that channel 1a does not contribute significantly to the overall reaction.

CH_2Cl_2 can be formed either directly in the substitution reaction channel 1b or indirectly via the formation of CH_2Cl radicals in channel 1c followed by their reaction with Cl_2. To distinguish between channels 1b and 1c, experiments were performed with O_2 added to the reaction mixtures. In the presence of Cl_2 and O_2, there is a competition for the available CH_2Cl radicals. If reaction channel (1c) is important, the formation of CH_2Cl_2 will be suppressed by addition of O_2. An experiment was performed using a mixture of 21 mTorr of CH_2ICl, 0.7 Torr of Cl_2 in 700 Torr of O_2. The observed products following UV irradiation were HC(O)Cl, CH_2ClOOH, and CO in a combined yield of 84 ± 7%: these are the expected products from reactions involving CH_2ClO_2 radicals in the chamber.[23] There was no observable CH_2Cl_2 formation (<8%) from which we derive an upper limit of $k_{1b}/k_1 < 0.08$.

To investigate the suppression of the CH_2Cl_2 yield with addition of O_2, a series of experiments were performed at 700 Torr total pressure. The partial pressures of CH_2ICl and Cl_2 were kept constant at 23 mTorr and 1.5 Torr while $[O_2]$ was varied from 203 to 1100 mTorr. The resulting yield of CH_2Cl_2 was in the range 18−46%. The results are plotted as triangles in Figure 6. As seen from Figure 6, there is no discernible difference between the observed variation of the CH_2Cl_2 yield with $[Cl_2]/[O_2]$ in experiments performed using $CH_2ICl/Cl_2/O_2$ and $CH_3Cl/Cl_2/O_2$ mixtures. This is a strong indication that the reaction of Cl atoms with CH_2ICl proceeds solely via reaction 1c.

Finally, experiments were performed at a reduced total pressure of 100 Torr of N_2 diluent. The triangles in Figure 8 show the observed yield of CH_2Cl_2 following UV irradiation of a mixture of 47 mTorr of CH_2ICl, 48 mTorr of O_2, and 0.2 Torr of Cl_2 in 100 Torr of N_2 diluent. The yield of CH_2Cl_2 was 49 ± 2%. Using the Troe expression derived in the previous section, it can be calculated that at 100 Torr $k_8/k_7 = 4.4$. In a mixture containing 48 mTorr of O_2 and 0.2 Torr of Cl_2 it follows that 49% of CH_2Cl radicals will react with Cl_2 while the remainder will react with O_2. The magnitude of the observed suppression of the CH_2Cl_2 yield on addition of O_2 is consistent with the reaction of Cl atoms with CH_2ICl proceeding exclusively via channel 1c at 100 Torr and 295 K.

The product data show that at 295 K and total pressures of 100−700 Torr the reaction of Cl atoms with CH_2ICl proceeds essentially 100% via iodine transfer to form CH_2Cl radicals and ICl. As discussed in the following section, the reaction may proceed via a short-lived adduct which is not visible in these FTIR experiments.

4. Conclusion

We present here the results of a study of the kinetics and mechanism of the reaction of Cl atoms with CH_2ICl. The reaction proceeds rapidly with a rate constant of 8.5×10^{-11} cm^3 $molecule^{-1}$ s^{-1} at 298 K to give CH_2Cl radicals and, by inference, ICl. The reaction has a small negative activation energy, suggesting the importance of long-range attractive forces in the detailed reaction dynamics. Such behavior is consistent with recent experimental work by Wine and co-workers,[24]

TABLE 2: Enthalpy Changes at 298 K for a Set of Reactions of the Type RX + Cl → R + XCl Where R = Methyl or a Halo-Substituted Methyl Group and X = Cl, Br, or I[a]

RX	XCl	ΔH_r (298 K) (kJ mol^{-1})
CH_3Cl	Cl_2	108 ± 1
CH_3Br	BrCl	76 ± 1
CH_3I	ICl[b]	26 ± 1
CH_2Cl_2	Cl_2	96 ± 8
CH_2BrCl[a]	BrCl	60 ± 17
CH_2ICl[a]	ICl[b]	2 ± 29
CH_2Br_2	BrCl	72 ± 8
$CHCl_3$	Cl_2	78 ± 8

[a] Heats of formation used to evaluate heats of reaction are taken from ref 12 unless otherwise indicated. [b] Heats of formation of CH_2ClBr and CH_2ClI are estimates based on group additivity, taken from ref 32. [c] Heat of formation of ICl is taken from ref 33.

showing that reactions of atomic chlorine with CH_3I, CH_3Br, CF_3CH_2I, and CD_3CD_2I proceed via two channels: adduct formation and direct hydrogen abstraction. Adduct formation rate constants are found to be much faster than the corresponding hydrogen abstraction rate constants, but the dominant fate of the weakly bound adducts in the experiments of Wine and co-workers was dissociation back to reactants.[24] Ab initio calculations by McKee[24c] predict 298 K adduct bond strengths similar to those measured by Wine and co-workers (ranging from 24.5 kJ mol^{-1} for $CH_3Br\cdots Cl$ to 59.l kJ mol^{-1} for $CD_3CD_2I\cdots Cl$). Similar calculations by Lazarou et al.[25] report the existence of stable adducts of Cl atoms with HI, CH_3I, and CH_3OCH_2I with 298 K bond strengths of 31.1, 52.4, and 51.3 kJ mol^{-1}, respectively. Recent studies of the reaction of F atoms with CF_2BrH, CH_2BrCl, and CH_3Br[26−28] have shown that adduct formation is also important in the reaction of F atoms with brominated methanes. It appears that the formation of short-lived adducts is a common facet of the reactions of F and Cl atoms with brominated and iodinated organic compounds.

Kinetic data for reactions of Cl atoms with a number of chloro- and bromo-substituted methanes have been reported in the literature. Room-temperature rate constants for Cl reactions with CH_3Cl, CH_2Cl_2, $CHCl_3$, CH_3Br, CH_2Br_2, and CH_2ClBr are all within the range $(1-5) \times 10^{-13}$ cm^3 molecule $^{-1}$ s^{-1} with hydrogen abstraction being the dominant reaction pathway;[12] activation energies for these reactions lie in the range 6.7−11.4 kJ mol^{-1}.[11] Formation of a weakly bound adduct has been observed for the $Cl+CH_3Br$ reaction,[24] and such adducts presumably can form in other Cl+haloalkane reactions as well; however, in most cases adduct formation appears to be rapidly reversible. The room-temperature rate constant for hydrogen abstraction from CH_3I by Cl is 8×10^{-13} cm^3 molecule $^{-1}$ s^{-1}.[24] The $CH_3I\cdots Cl$ adduct is more strongly bound than are Cl adducts with chloro- or bromo methanes, but in the absence of scavengers, its primary fate is dissociation back to $Cl+CH_3I$.[24] The room-temperature rate constant reported in this study for nonreversible channels of the $Cl+CH_2ClI$ reaction is 100−800 times faster than those of the Cl+haloalkane reactions discussed above, and the dominant reaction pathway is halogen transfer as opposed to hydrogen transfer for the reactions discussed above. The heats of reaction for halogen transfer channels in Cl reactions with the halomethanes discussed above are listed in Table 2. The atypical kinetic behavior observed for the $Cl+CH_2ICl$ reaction can be rationalized on thermochemical grounds. Production of dihalogen products from Cl reactions with CH_3Cl, CH_2Cl_2, $CHCl_3$, CH_3Br, CH_2Br_2, CH_2ClBr, and CH_3I is endothermic in all cases; hence, the energetically most favorable pathway for adduct decomposition is back to Cl+halomethane reactants. Formation of $CH_2Cl+ICl$ from the $Cl+CH_2ICl$ reaction is apparently exothermic (based upon the rapid observed reaction); hence, the energetically most favorable pathway for $CH_2ClI\cdots Cl$ decomposition is to $CH_2Cl+ICl$, not to $CH_2ICl+Cl$.

Since the $Cl+CH_2ICl$ reaction is very fast, its potential role as an atmospheric degradation mechanism for CH_2ICl warrants consideration. The atmospheric photolysis rate of CH_2ICl has recently been evaluated by Rattigan et al.;[6] a value of 2×10^{-5} s^{-1} appears typical for the tropical and midlatitude marine boundary layer. Establishing chlorine atom concentrations in the marine boundary layer is a topic of much current interest within the atmospheric chemistry community. The best estimates currently available suggest that typical marine boundary layer levels of Cl atoms are around 10^4/cm^{-3},[29−31] although the uncertainty in this estimate remains rather high. Using this estimate in conjunction with the value $k_1 = 8.5 \times 10^{-11}$ cm^3 molecule $^{-1}$ s^{-1} reported in this study gives a pseudo-first-order rate constant of 8.5×10^{-7} s^{-1} for CH_2ICl destruction via reaction with Cl. Hence, reaction 1 will compete with photolysis as an atmospheric destruction mechanism for CH_2ICl only if the average marine boundary layer concentration of Cl atoms is near the high end of the range of possible values. There are no kinetic data in the literature for the $OH + CH_2ICl$ reaction. For this reaction to be important as an atmospheric destruction mechanism for CH_2ICl, its rate constant would have to be much faster than the known rate constants for OH reactions with CH_3I and CF_3I (7.2×10^{-14} and 3.1×10^{-14} cm^3 molecule $^{-1}$ s^{-1} at 298 K, respectively[11]).

Acknowledgment. Research at Georgia Tech was supported by Grants NAGW-1001 and NAG5-3634 from the National Aeronautics and Space Administration-Upper Atmosphere Research Program.

References and Notes

(1) Davis, D.; Crawford, J.; Liu, S.; McKeen, S.; Bandy, A.; Thornton, D.; Rowland, F.; Blake, D., *J. Geophys. Res.* **1996**, *101*, D1, 2135.

(2) Chameides, W. L., Davis, D. D., *J. Geophys. Res.* **1980**, *85*, C12, 7383.

(3) Solomon, S., Rolando, R. G., Ravishankara, A. R., *J. Geophys. Res.* **1994**, *99*, D10, 20, 491.

(4) Moore R. M., Tokarczyk, *J. Geophys. Res.* **1992**, *19*, 1779.

(5) Class, T. H.; Ballschmiter, K. *J. Atmos. Chem.* **1988**, *6*, 35.

(6) Rattigan, O. V.; Shallcross, D. E.; Cox, R. A., *J. Chem. Soc., Faraday Trans.* **1997**, *93*, 2839.

(7) Roehl, C. M.; Burkholder, J. B.; Moortgat, G. K.; Ravishankara, A. R.; Crutzen, P. J. *J. Geophys. Res.* **1997**, *102*, 12819.

(8) Wallington, T. J.; Japar, S. M. *J. Atmos. Chem.* **1989**, *9*, 399.

(9) Nicovich, J. M.; Wang, S.; McKee, M. L.; Wine, P. H. *J. Phys. Chem.* **1996**, *100*, 680 and references therein.

(10) Stated minimum purity of liquid phase in high-pressure cylinder.

(11) Wallington, T. J.; Hurley, M. D. *Chem. Phys. Lett.* **1992**, *189*, 437.

(12) DeMore, W. B.; Sander, S. P.; Golden, D. M.; Hampson, R. F.; Kurylo, M. J.; Howard, C. J.; Ravishankara, A. R.; Kolb, C. E.; Molina, M. J., Evaluation No. 12, Jet Propulsion Laboratory Publication 97-4; Jet Propulsion Laboratory: Pasadena, CA, 1997 and references therein.

(13) Busch, G. E.; Mahoney, R. T.; Morse, R. I.; Wilson, K. R. *J. Chem. Phys.* **1969**, *51*, 449.

(14) Park, J.; Lee, Y.; Flynn, G. W. *Chem. Phys. Lett.* **1991**, *186*, 441.

(15) Tyndall, G. S.; Orlando, J. J.; Kegley-Owen, C. S., *J. Chem. Soc., Faraday Trans.* **1995**, *91*, 3055.

(16) Fletcher, I. S.; Husain, D. *Chem. Phys. Lett.* **1977**, *49*, 516.

(17) Clark, R. H.; Husain, D. *J. Photochem.* **1983**, *21*, 93.

(18) Chichinin, A. I.; Krasnoperov, L. N. *Chem. Phys. Lett.* **1989**, *160*, 448.

(19) Seetula, J. A.; Gutman, D.; Lightfoot, P. D.; Rayez, M. T.; Senkan, S. M. *J. Phys. Chem.* **1991**, *95*, 10688.

(20) Braun, W.; Herron, J. T.; Kahaner, D. K. *Int. J. Chem. Kinet.* **1988**, *20*, 51.

(21) Fenter, F. F.; Lightfoot, P. D.; Caralp, F.; Lesclaux, R.; Niiranen, J. T.; Gutman, D. *J. Phys. Chem.* **1993**, *97*, 4695.

(22) Troe, J. *J. Phys. Chem*. **1979**, *83*, 114.

(23) Kaiser, E. W.; Wallington, T. J. *J. Phys. Chem*. **1994**, *98*, 5679

(24) (a) Wine, P. H. Presented at the 210th National ACS Meeting in Chicago, August, 1995. (b) Piety, C. A. Thesis, Georgia Institute of Technology, **1996**. (c) Piety, C. A.; Nicovich, J. M.; Ayhens, Y. V.; Estupinan, E. G.; Soller, R.; McKee, M. L.; Wine, P. H. Paper D6, Presented 14th Symposium on Gas Kinetics, Leeds, United Kingdom, **1996**.

(25) Lazarou, Y. G.; Kambanis, K. G.; Papagiannakopoulos, P. *Chem. Phys. Lett.* **1997**, *268*, 498.

(26) Bilde, M.; Sehested, J.; Møgelberg, T. E.; Wallington, T. J.; Nielsen O. J. *J. Phys. Chem.* **1996**, *100*, 7050.

(27) Bilde, M.; Sehested, J.; Nielsen, O. J.; Wallington, T. J. *J. Phys. Chem. A* **1997**, *101*, 5477.

(28) Sehested, J., Bilde, M.; Møgelberg, T. E.; Wallington, T. J.; Nielsen, O. J. *J. Phys. Chem*. **1996**, *100*, 10989.

(29) Pszenny, A. A. P.; Keene, W. C.; Jacob, D. J.; Fan, S.; Maben, J. R.; Zetwo, M. P.; Springer-Young, M.; Galloway, J. N. *Geophys. Res. Lett*. **1993**, *20*, 699.

(30) Singh, H. B.; Thakur, A. N.; Chen, Y. E.; Kanakidou, M. *Geophys. Res. Lett.* **1996**, *23*, 1529.

(31) Vogt, R.; Crutzen, P. J.; Sander, R. *Nature* **1996**, *383*, 327.

(32) Kudchadker, S. A.; Kudchadker, A. P. *J. Phys. Chem. Ref. Data* **1978**, *7*, 1285.

(33) Lias, S. G.; Bartmess, J. E.; Liebman, J. R.; Holmes, J. L.; Levin, R. D.; Mallard, W. G. *J. Phys. Chem. Ref. Data* **1988**, 17 (Suppl. 1).